Lighting gel filters as low-cost alternatives for fluorescence imaging and optical system design

Alberto J. Ruiz,[a,*] **Mia K. Giallorenzi**,[a] **Brady Hunt**,[a] **Kimberley S. Samkoe**,[a,b] **and Brian W. Pogue**[a,c]

[a]Thayer School of Engineering, Dartmouth College, Hanover, New Hampshire, United States
[b]Geisel School of Medicine, Department of Surgery, Hanover, New Hampshire, United States
[c]University of Wisconsin–Madison, Department of Medical Physics, Madison, Wisconsin, United States

Abstract. Lighting gel filters are widely used in commercial industries, but their adoption in scientific applications is limited, despite their low cost and form factor advantages. Here, we compare the optical performance of lighting gel filters to commonly used dielectric and colored glass filters in terms of absorbance spectra, passband transmission, angle of incidence dependence, autofluorescence, and photostability. Further comparison is performed in both preclinical and clinical imaging applications. The results show that gel filters might be a superior filter choice in several optical systems, including compact designs and fluorescence imaging applications. Compact designs using gel filters could have a significant advantage for applications such as point-of-care diagnostics, smartphone device add-ons, and single-use fluorescent assays. [DOI: 10.1117/1.OE.61.8.085103]

Keywords: filters; lighting gel filters; low-cost; fluorescence; imaging; smartphone; optical filtering.

Paper 20220533G received May 21, 2022; accepted for publication Aug. 1, 2022; published online Aug. 22, 2022.

1 Introduction

Lighting gel filters have been used over the past 100 years to modify the color of traditional light sources and are widely adopted in the photography, film, and performance arts industries. Modern gel filters are manufactured using surface-coated polyester film (PET), deep-dyed PET, or body-colored polycarbonate.[1] Few uses of gel filters have been recorded in scientific literature (the authors found only three instances), which include their use as optical filters for fluorescent protein and dye screening,[2] observation of fluorescence quenching mechanisms,[3] and production of complex lighting patterns using laser cutting techniques.[4] The main advantages of gel filters are their low cost and form-factor customization that results from their mechanical flexibility, thin profile (~0.1-mm thick), and ability to be laser cut. We hypothesize that the lack of comprehensive optical characterization and comparison to commonly used dielectric and colored glass filters has hampered the use of gel filters in scientific applications. The adoption of gel filters in optical designs could have a significant impact on point-of-care diagnostics,[5] including low-cost smartphone imaging systems,[6] and disposable lab-on-chip fluorescence tests.[7] Additional applications include miniaturization of optical designs,[8,9] colorimetric imaging,[10] and low-cost educational tools.[11]

This study aims to identify the potential advantages and disadvantages of using lighting gel filters in scientific applications. In this paper, we focused on long-pass filtering for fluorescence applications, comparing gel filter blocking optical density (OD), passband transmission, angle

*Address all correspondence to Alberto J. Ruiz, alberto.j.ruiz.th@dartmouth.edu

of incidence (AOI) dependence, auto-fluorescence, and photo-reliability performance to that of dielectric and colored glass filters. Furthermore, a case study of direct performance comparison between dielectric and gel filters is performed for calibration, preclinical, and clinical measurements within a smartphone-based fluorescence imager. The results show that gel filters can serve as viable alternatives for optical filtering, particularly when cost and form factor are prioritized in the optical system design. The main drawbacks of using gel filters are their lack of specifications for optical blocking efficacy, lower transmission, and longer transition ranges, requiring careful characterization to determine if they meet each optical system's performance requirements.

2 Methods

Long-pass dielectric, glass, and gel filters with cut-on wavelengths of 400, 500, and 600 nm were used to evaluate optical performance differences [Fig. 1(a)]. The filters are characterized using a spectrophotometer, fluorospectrometer, and photo-reliability system [Figs. 1(b)–1(d)].

The blocking OD, passband transmission, long-pass transition range, and the AOI dependence of optical spectra for all filters were measured using a Cary 50 UV-VIS spectrophotometer. Spectrophotometer scans were performed from 200 to 900 nm with a 1-nm step size. AOI tests were performed at 0 deg and 45 deg. Autofluorescence resulting from a 380-nm excitation was measured using the Horiba Fluoromax 4 fluorospectrometer. Photo-reliability tests were performed using a high irradiance 395-nm collimated LED (70 mW/cm^2 at the filter surface). The LED transmitted power was monitored over a 1-h interval using a Thorlabs S120VC photodiode sensor. Omega optical dielectric filters (400LP, 500LP, and 600LP), Thorlabs colored glass filters (FGL400, FGL495, and FGL610), Rosco E226 gel filter, and LEE Oklahoma yellow (OKY) and AS Golden Amber (ASGA) gel filters were compared. Custom three-dimensional printed holders were used to mount the filters in the respective measurement device.

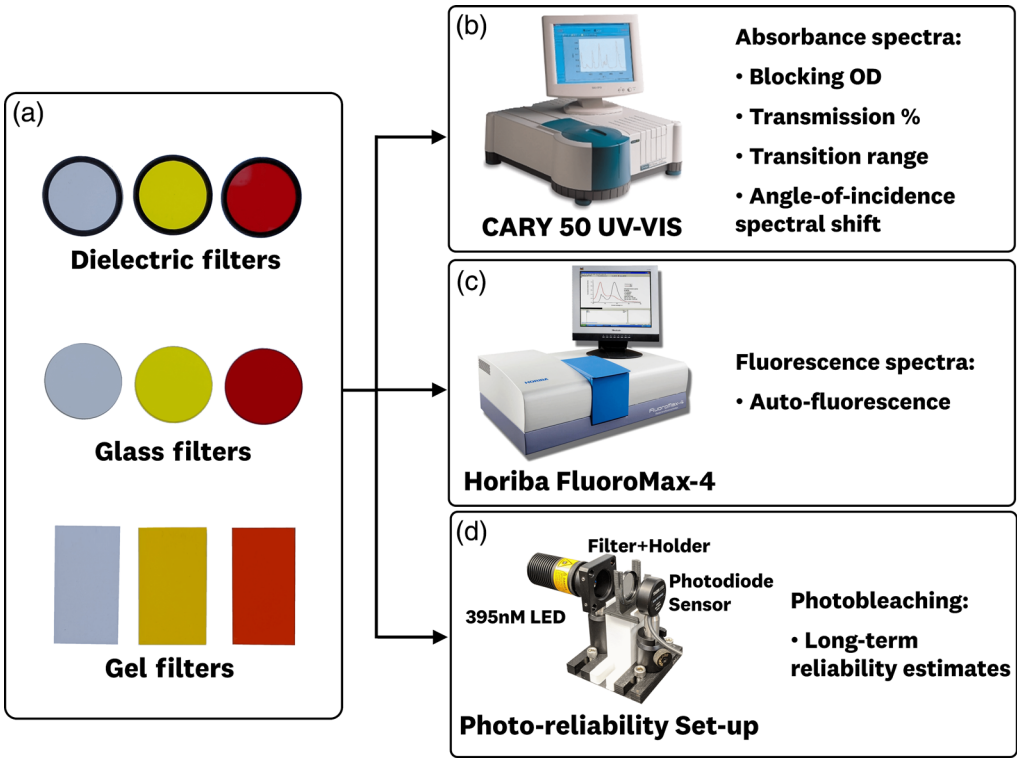

Fig. 1 Overview of filter comparison tests. (a) Long-pass (400, 500, and 600 nm) dielectric, glass, and gel filters are used for comparing optical performance. The filters were characterized using a (b) spectrophotometer, (c) fluorospectrometer, and (d) photo-reliability testing system.

The use of gel filters in fluorescence imaging was evaluated by comparing the 600LP dielectric and ASGA gel filter performance in a previously published smartphone-based system designed for quantitative detection of protoporphyrin IX (PpIX).[6,12] Sensitivity of fluorescence detection for each filter configuration was measured by imaging of serial dilutions of PpIX. The unprocessed pixel signal (12 bit) versus PpIX concentrations were obtained by imaging 1% Intralipid solutions with varying PpIX concentrations in the 30 to 1000 nM range. To assess the performance of *in-vivo* fluorescence capture, preclinical and clinical measurements were completed using both filter configurations. Preclinical measurements of PpIX incubation at 10 min and 1 h were performed in an athymic nude mouse by topical application of a 10% aminolevulinic acid (ALA) gel (Ameluz, Biofrontera Inc., Germany). Clinical measurements were performed by applying the 10% ALA gel on the arm of consented patients, followed by a 3 h incubation with the site occluded with plastic wrap. All animal and human imaging were performed following protocols approved by the Dartmouth College Institutional Review Board. The reported fluorescence image quality metric for the filter comparison, contrast-to-variability ratio (CVR), is defined as $\mathrm{CVR} = (I^{\mathrm{FL}}_{\mathrm{ALA}} - I^{\mathrm{FL}}_{\mathrm{Control}})/\sqrt{\sigma^2_{\mathrm{ALA}} + \sigma^2_{\mathrm{Control}}}$, where $I^{\mathrm{FL}}_{\mathrm{ALA}}$ and $I^{\mathrm{FL}}_{\mathrm{Control}}$ are the averaged fluorescence intensities in the imaged ALA-applied area and the control area, alongside their respective variances σ^2_{ALA} and $\sigma^2_{\mathrm{Control}}$.[13] The CVR metric is preferred over standard signal-to-noise calculations as it provides a better estimation of fluorescence contrast performance by accounting for the signal and variance of both the fluorescence and control regions in the metric calculation.[14]

3 Results

3.1 *Optical Density and Transmission*

Figure 2 shows the OD measurements and corresponding transmission spectra ($T = 10^{-\mathrm{OD}}$) of the different filters. Measurements of the 400-nm filters [Fig. 2(a)] show that the gel filter's OD blocking spectra closely matched the dielectric filter's performance and was superior to the colored glass filter. Similar transmission spectra performance was observed between the glass and gel filter, with the dielectric filter providing ~5% to 10% greater transmission in the passband regime.

The 500-nm filter measurements [Fig. 2(b)] show a variation in the OD spectrum of the gel filter, which corresponds to a small "bump" in the transmission spectra. Furthermore, the gel filter exhibited a longer transition range. The dielectric and glass filter performance is closely matched.

The 600-nm filter measurements [Fig. 2(c)] demonstrate a significantly longer transition range for the gel filter as well as a small variation within its OD spectrum. The dielectric and glass filters are closely matched in performance.

3.2 *Angle of Incidence Dependence*

Figure 3 displays the filters' angle-of-incidence dependence measurements (at 0 deg and 45 deg). The dielectric filters [Fig. 3(a)] show significant blue shifts of 25.4, 39.4, and 53.9 nm for the 400, 500, and 600 nm filters, respectively. This result is expected given the optical interference mechanism used in dielectric filter design, which is sensitive to the optical path length changes. In contrast, the glass [Fig. 3(b)] and gel [Fig. 3(c)] filters showed no significant shifts in their transmission spectra.

3.3 *Filter Autofluorescence*

Autofluorescence measurements are shown in Fig. 4. The 400-nm filter measurements [Fig. 4(a)] showed that the dielectric and gel filters exhibited low levels of autofluorescence while the glass filter had ~2 orders of magnitude greater autofluorescence. The 500- and 600-nm filter measurements [Figs. 4(b) and 4(c)] display the same trends: comparable low autofluorescence

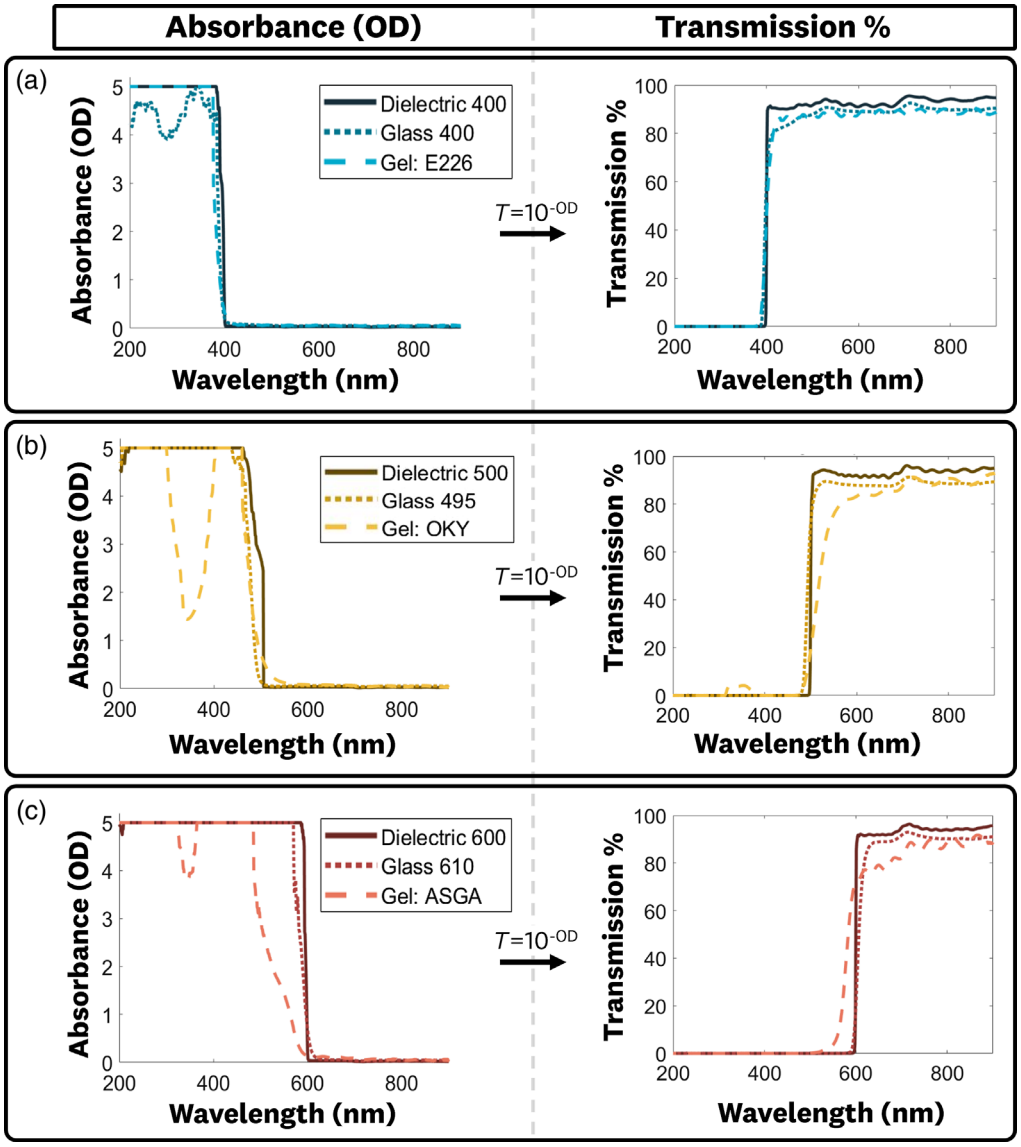

Fig. 2 Spectrophotometer measurements of OD and transmission. (a) 400-nm long-pass filter results, showing comparable performance between the gel and dielectric filters, (b) 500-nm long-pass filter results, showing a variable OD for the stopband of the gel filter, and (c) 600-nm long-pass filter results, showing longer transition range of the gel filter.

for dielectric and gel filters in contrast to one to two orders of magnitude higher signal from the glass filters. These results match the known high autofluorescence behavior of colored glass filters.[15]

3.4 *Filter Photo-Reliability*

The results of the photo-reliability test are shown in Fig. 5. The 400-nm filter measurements [Fig. 5(a)] demonstrate flat transmission responses from the gel and dielectric filters over the 1-h test. The glass filter exhibits an initial decrease in transmission before stabilizing. Similar patterns are observed for the 500 nm [Fig. 5(b)] and 600 nm [Fig. 5(c)] filter measurements. The dielectric and gel filters' flat response suggest that no degradation was observed over the 1-h test. The reliability curves of the glass filters are reproducible for all three filters, where room temperature cooling followed by a repetition of the photo-reliability experiment results in the same initial decrease in the transmitted signal; this indicates that the glass filters did not experience

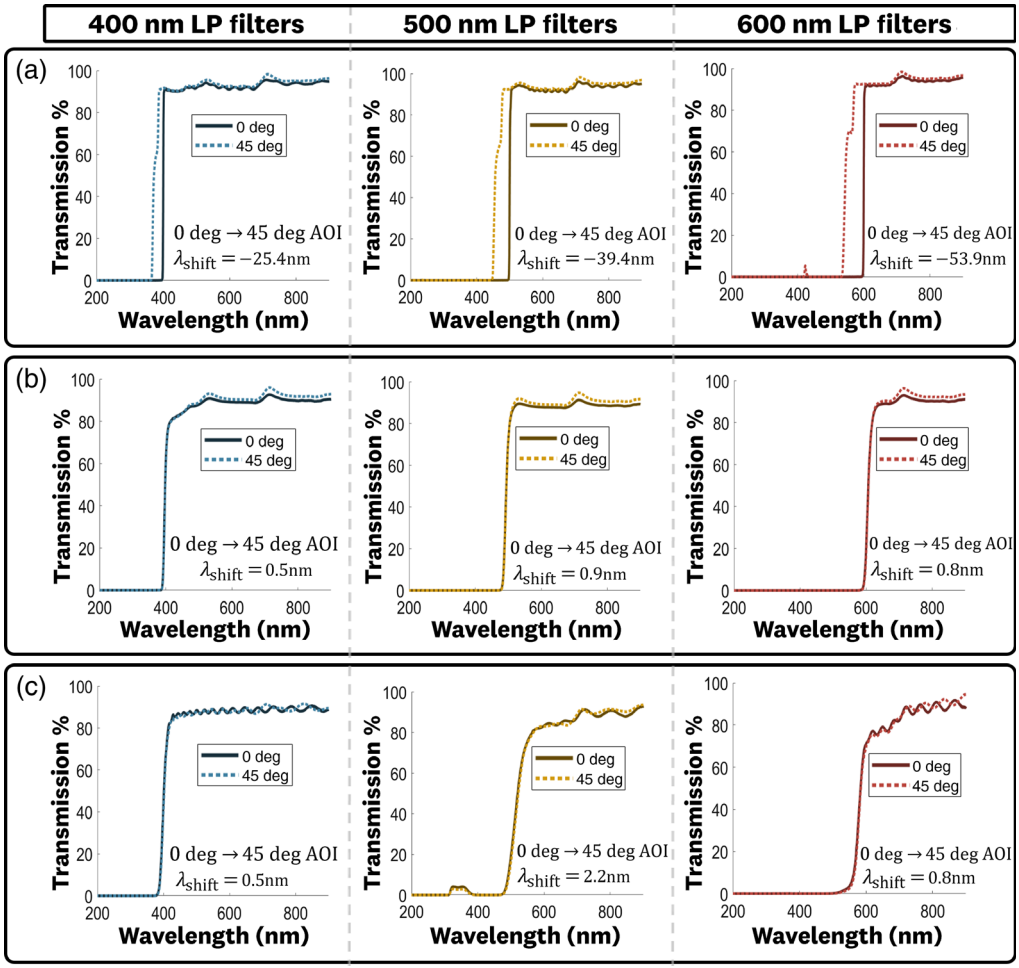

Fig. 3 AOI measurements to determine spectral dependence. (a) Dielectric filters show significant spectral shifts with a change in AOI; (b) and (c) glass and gel filters show minimal shifts in spectral features.

any degradation during testing and that the initial decrease could be related to thermal effects from the high irradiance of the 395-nm LED.

3.5 *Gel Filter Fluorescence Imaging Performance Evaluation*

Figure 6 shows the results of using the 600LP dielectric and Lee ASGA gel as emission filters within a smartphone-based fluorescence imager.[6] The imaging system [Fig. 6(a)] is designed to quantify PpIX using 405-nm LEDs for excitation and an emission filter for fluorescence signal isolation (600 to 700 nm). Varying concentrations of PpIX in 1% Intralipid solution were imaged with each filter configuration to generate pixel intensity versus concentration calibration curves [Figs. 6(b) and 6(c)]. The dielectric filter [Fig. 6(b)] and gel filter [Fig. 6(c)] calibrations indicate that both device configurations were sensitive in the 30 to 1000 nM PpIX concentration range with a goodness of fit of $R^2 > 0.99$. Imaging of *in-vivo* accumulation of PpIX was performed on mice [Figs. 6(e)–6(i)] and humans [Figs. 6(j)–6(l)] using both filter configurations. Both configurations were able to image the *in-vivo* PpIX fluorescence for both the preclinical and clinical settings. The calculated CVR for the mice and human arm images was $\mathrm{CVR}_{\mathrm{gel}}^{\mathrm{mice}} = 4.6$, $\mathrm{CVR}_{\mathrm{gel}}^{\mathrm{arm}} = 1.6$, $\mathrm{CVR}_{\mathrm{die}}^{\mathrm{mice}} = 5.3$, and $\mathrm{CVR}_{\mathrm{die}}^{\mathrm{arm}} = 2.1$. Despite its longer transition range and lower passband transmission, the gel filter matched the dielectric filter performance within the Intralipid + PpIX calibration test, with the dielectric filter configuration providing a 17% and 30% higher CVR in the mice and human measurements, respectively.

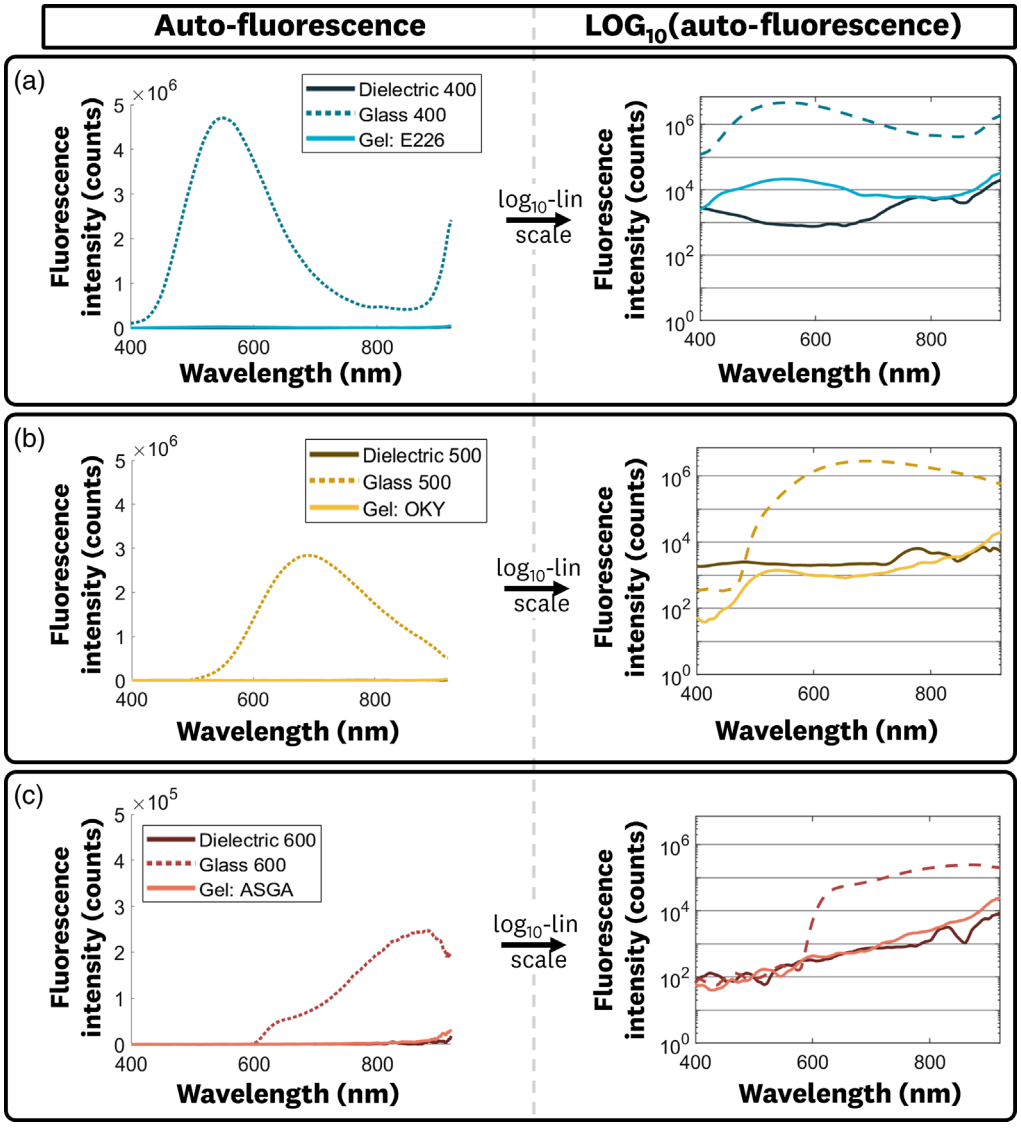

Fig. 4 Filter autofluorescence measurements using 380-nm excitation. The (a) 400 nm, (b) 500 nm, and (c) 600 nm filter measurements show that glass filters exhibit one to two orders of magnitude greater autofluorescence when compared to the dielectric and gel filters.

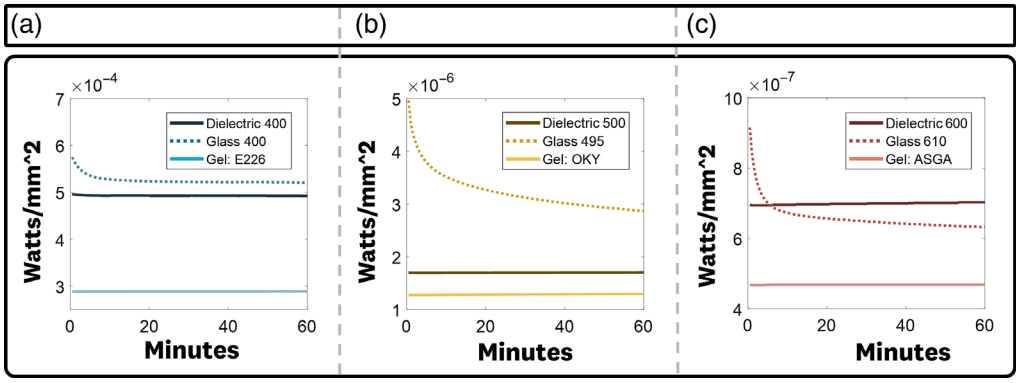

Fig. 5 Photo-reliability measurements for the (a) 400 nm, (b) 500 nm, and (c) 600 nm filter sets.

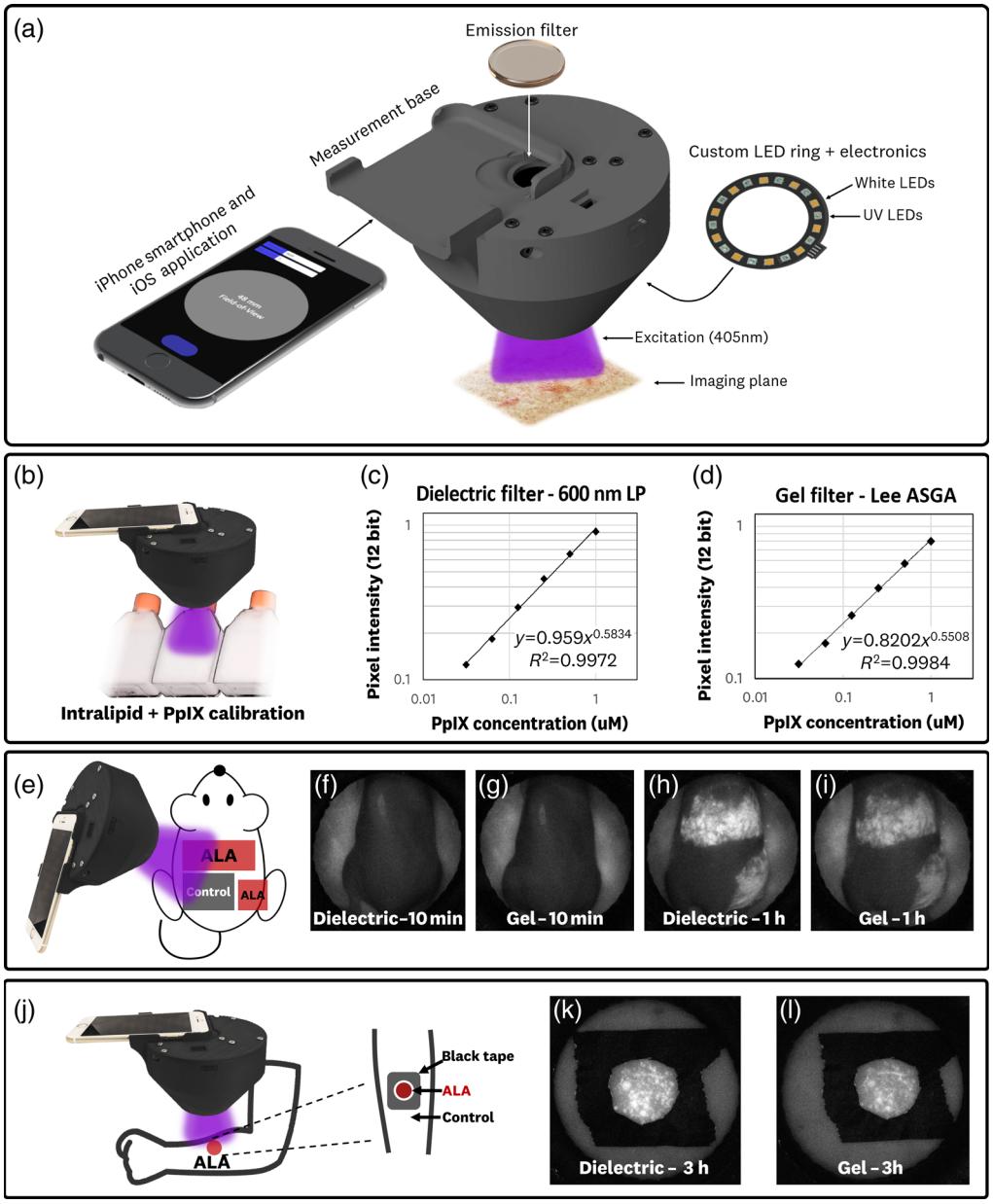

Fig. 6 Dielectric versus gel filter comparison using a smartphone-based fluorescence imager. (a) The smartphone-based imager uses 405-nm excitation and a long-pass emission filter to detect PpIX fluorescence. (b) Fluorescence intensity calibration for varying PpIX concentrations using (c) 600LP dielectric filter and (d) Lee ASGA gel filter. (e–f) Preclinical measurements of incubated PpIX fluorescence in mice. (j–l) Clinical measurements of incubated PpIX fluorescence. All fluorescence images are displayed using the same intensity scale.

4 Discussion

This work is the first to rigorously characterize the optical performance of lighting gel filters and compare them to other commercially available optical filters. A tabular summary of the results from these comparisons is shown in Fig. 7. Overall, gel filters provide a unique set of advantages, including cost, shape customization, and a combination of low autofluorescence and AOI independence, making them a viable alternative in optical system design.

The spectrophotometer measurements in Fig. 2 demonstrated the potential of lighting gel filters to match dielectric and colored glass filters' optical performance, exhibiting blocking ODs of 5+ and transmissions $> 85\%$ for the passband region. Drawbacks for the gel filters

	Dielectric	Glass	Gel
Cost	Expensive ✗	Less Expensive ✗	Low Cost ✓
Shape customization	No ✗	Limited ✗	Yes ✓
Specifications	Yes ✓	Yes ✓	Limited ✗
Spectral tunability	Yes ✓	Limited ✗	Very limited ✗
Transition range	Shortest ✓	Shorter ✗	Longest ✗
Transmission %	High ✓	Variable ✗	Variable ✗-✗
Blocking OD	Good ✓	Good ✓	Variable ✗
Angle of incidence dependence	Large ✗	Small ✓	Small ✓
Auto-fluorescence	Low ✓	High ✗	Low ✓
Long term reliability	Good ✓	Good ✓	Good ✓

Fig. 7 Qualitative summary of performance metrics for dielectric, colored glass, and lighting gel filters.

included longer transition ranges, variable OD spectra, and slightly lower transmission; these factors should be carefully considered in the optical system design. OD and transmission spectra for 17 additional gel filters were also tested, showing similar characteristics to the comparison test filters.

The AOI dependence measurements in Fig. 3 demonstrated the significant spectral shifts of dielectric filters, which should be considered in applications where a wide range of incidence angles will be encountered. For example, the smartphone-based camera system calibration comparison [Figs. 6(b)–6(d)] showed noticeable spectral vignetting for the images collected using the 600LP dielectric filter. In contrast, the gel and glass filters showed minimal spectral shifts, making them better candidates for imaging applications that do not require the short transition ranges or spectral specificity of dielectric filters.

Autofluorescence measurements in Fig. 4 showed low signal levels for dielectric and gel filters. Glass filters showed one to two orders of magnitude higher autofluorescence, resulting in potentially significant decreases in the signal-to-noise ratio, particularly for applications with low levels of fluorescence signal. Combined with the AOI dependence measurements, these results demonstrate the potential of using gel filters for low-cost fluorescence system design, including smartphone imaging, fiber-based probes, and single-use fluorescent assays.

The gel filters' ability to match the photo-reliability performance of dielectric filters in Fig. 5 correlates with their designed use with traditional light sources, which involve high irradiance and elevated temperatures. Based on these results, gel filters would be expected to have a long-term reliability performance comparable to dielectric filters. However, testing long-term reliability in the intended application would be warranted, given that gel filter manufacturers do not provide specific long-term reliability performance regarding lighting power, heat, UV exposure, etc. The provided reliability specifications are normally limited to maximum operating temperatures; as an example, the tested gel filters had a 180°C maximum specification.

Generally, the differences observed between the three filter types are due to the underlying optical mechanisms and filter substrates. Dielectric filters are normally manufactured through layering of glass and dielectric material that are tuned for optical interference. Colored glass and gel filters rely on the absorption of light through the incorporation of absorbers in a glass substrate or thin polymers, respectively.

The dielectric and gel comparison within a smartphone-based PpIX fluorescence imager (Fig. 6) showed the ability of the gel filter to serve as a low-cost replacement in both preclinical and clinical imaging applications. For the tested device, the replacement of the 600LP dielectric filter with the Lee ASGA gel filter would result in a ~50% reduction in the total build-of-

materials cost. Although the gel filter configuration was able to successfully image the PpIX accumulation in mice and humans, its lower transmission and longer transition range resulted in lower CVRs when compared to the dielectric filter. This lower contrast should be considered in applications that have lower signal levels, such as imaging of PpIX accumulation with shorter incubation times.

The main disadvantages of gel filters are the limited availability of OD performance specifications, longer transition ranges, and lower passband transmissions. These disadvantages complicate the application-specific suitability of gel filters, such that optical characterization within the intended operating conditions would be necessary to determine if the required performance parameters are met.

Given the < 0.1 mm thickness of gel filters, future studies could explore the stacking of gel filters to customize spectral features, including increased OD. The simultaneous use of bandpass and long-pass features of gel filters within a single optical design could also be explored. In conjunction with this study, we developed a low-cost, ultracompact attachment for smartphone fluorescence imaging that was enabled by implementing lighting gel filters in the optical design.[16]

5 Conclusion

Optical characterization and comparison to conventional optical filters demonstrated the ability of gel filters to serve as viable alternatives in optical system design. Leveraging the low-cost and shape customization advantages of gel filters could significantly impact the development of single-use fluorescent assays and point-of-care imaging tools. Given the variable optical properties, coupled with limited availability of specifications, careful characterization of gel filters is required for proper implementation within an optical system design.

Acknowledgments

Thayer School of Engineering at Dartmouth. Henry Luce Foundation and its Clare Boothe Luce Fellowship (MG). The authors declare no conflict of interests.

References

1. K. Billington et al., *The Rosco Guide to Color Filters*, p. 20, Rosco Laboratories Inc. (2011).
2. J. R. Heil, R. F. Nordeste, and T. C. Charles, "The fluorescence theatre: a cost-effective device using theatre gels for fluorescent protein and dye screening," *Can. J. Microbiol.* **57**(4), 339–342 (2011).
3. C. S. Ball et al., "Quenching of unincorporated amplification signal reporters in reverse-transcription loop-mediated isothermal amplification enabling bright, single-step, closed-tube, and multiplexed detection of RNA viruses," *Anal. Chem.* **88**(7), 3562–3568 (2016).
4. E. Rawn and J. Li, "Laser cut layered gels for lighting design," in *Extended Abstr. of the 2020 CHI Conf. Hum. Factors in Comput. Syst.*, ACM, Honolulu, Hawaii, pp. 1–7 (2020).
5. H. Zhu et al., "Optical imaging techniques for point-of-care diagnostics," *Lab Chip* **13**(1), 51–67 (2013).
6. A. J. Ruiz et al., "Smartphone fluorescence imager for quantitative dosimetry of protoporphyrin-IX-based photodynamic therapy in skin," *J. Biomed. Opt.* **25**(6), 063802 (2019).
7. A. Pais et al., "High-sensitivity, disposable lab-on-a-chip with thin-film organic electronics for fluorescence detection," *Lab Chip* **8**(5), 794 (2008).
8. F. L. Kiechle and C. A. Holland, "Point-of-care testing and molecular diagnostics: miniaturization required," *Clin. Lab. Med.* **29**(3), 555–560 (2009).
9. B. Dai et al., "Colour compound lenses for a portable fluorescence microscope," *Light Sci. Appl.* **8**(1), 75 (2019).

10. G. Sharma and H. J. Trussell, "Digital color imaging," *IEEE Trans. Image Process.* **6**(7), 901–932 (1997).
11. OSA Rochester Section, *The Optics Suitcase - Educational Outreach Presentation Guide*, The Optical Society (OSA) (2018).
12. A. J. Ruiz et al., "Smartphone-based fluorescence imager for PpIX-based PDT treatment planning: System design and initial results," *Proc. SPIE* **10860**, 108600R (2019).
13. N. Sadeghipour et al., "Prediction of optimal contrast times post-imaging agent administration to inform personalized fluorescence-guided surgery," *J. Biomed. Opt.* **25**(11), 116005 (2020).
14. K. M. Tichauer et al., "Task-based evaluation of fluorescent-guided cancer surgery as a means of identifying optimal imaging agent properties in the context of variability in tumor- and healthy-tissue physiology," *Proc. SPIE* **11222**, 112220O (2020).
15. J. Reichman, *Handbook of Optical Filters for Fluorescence Microscopy*, Chroma Technology Corporation (2000).
16. B. Hunt et al., "Ultracompact fluorescence smartphone attachment using built-in optics for protoporphyrin-IX quantification in skin," *Biomed. Opt. Express* **12**(11), 6995 (2021).

Alberto J. Ruiz recently completed his PhD and innovation fellowship at the Optics in Medicine Lab at Dartmouth College. He received his BS degree in applied physics from Harvey Mudd College in 2014. He has worked as an applications engineer at Thorlabs, Inc., and as an applications engineering manager at Cree, Inc. He is passionate about translational technologies, education, and social responsibility. His current research interests include photodynamic therapy, fluorescence-guided surgery, and low-cost optical system design.

Mia K. Giallorenzi is an undergraduate student at Thayer School of Engineering at Dartmouth, focusing on biomedical applications. As a Clare Boothe Luce Fellow, she conducted most of the experimental design, data acquisition, and analysis presented in this paper. She is passionate about science, languages, and the outdoors.

Brady Hunt is a research scientist at Thayer School of Engineering at Dartmouth, where he is developing optical systems for treatment guidance in dermatology and radiotherapy applications. He completed his doctorate degree under the mentorship of Rebecca Richards-Kortum at Rice University, contributing significant clinical assessments of point-of-care imaging technologies in medically underserved populations in Brazil. Prior to that, he graduated magna cum laude with his bachelor's degree in biophysics from Brigham Young University.

Kimberley S. Samkoe is an associate professor of engineering at Dartmouth College. She holds degrees in biochemistry and biophysical chemistry. She directs a prestigious National Cancer Institute R37 MERIT Award to develop paired-agent imaging principles in fluorescence-guided head and neck cancer surgery and is a key investigator in the ABY-029 clinical translational project at Dartmouth. She has published more than 60 peer-reviewed articles and holds additional funding from the Mark Foundation and a Faculty Award at Dartmouth-Hitchcock.

Brian Pogue is the editor-in-chief of the *Journal of Biomedical Optics*, and the chair of the Department of Medical Physics at the University of Wisconsin-Madison, and an adjunct professor at Dartmouth College. His work is in the role of optics in medicine, within biomedical engineering and medical physics, radiation therapy dosimetry, molecular-guided surgery, photodynamic therapy, and optically activated therapies. He has published more than 400 peer-reviewed publications at the intersection of optics, imaging, therapy, and cancer.